LANGMUIR Article
Cite This: Langmuir 2017, 33, 12989-12999
pubs.acs.org/Langmuir

L-Carnosine-Derived Fmoc-Tripeptides Forming pH-Sensitive and Proteolytically Stable Supramolecular Hydrogels

Rita Das Mahapatra,[†] Joykrishna Dey,*[,†] and Richard G. Weiss[‡]

[†]Department of Chemistry, Indian Institute of Technology Kharagpur, Kharagpur 721 302, India

[‡]Department of Chemistry and Institute for Soft Matter Synthesis and Metrology, Georgetown University, Washington, D.C. 20057-1227, United States

Supporting Information

ABSTRACT: A series of β-amino acid containing tripeptides has been designed and synthesized in order to develop oligopeptide-based, thermoreversible, pH-sensitive, and proteolytically stable hydrogels. The Fmoc [*N*-(fluorenyl-9-methoxycarbonyl)]-protected tripeptides were found to produce hydrogels in both pH 7 and 2 buffers at a very low concentration (<0.2% w/v). It has been shown that the Fmoc group plays an important role in the gelation process. Also a dependence of gelation ability on hydrophobicity of the side chain of the Fmoc-protected α-amino acid was observed. The effect of the addition of inorganic salts on the gelation process was investigated as well. Spectroscopic studies indicated formation of J-aggregates through $\pi-\pi$ stacking interactions between Fmoc groups in solution as well as in the gel state. In the gel phase, these self-assembling tripeptides form long interconnected nanofibrils leading to the formation of 3-dimensional network structure. The hydrogels were characterized by various techniques, including field emission electron microscopy, transmission electron microscopy, atomic force microscopy, rheology, Fourier transform IR, circular dichroism (CD), and wide-angle X-ray diffraction (WAXD) spectroscopy. The CD studies and WAXD analyses show an antiparallel β-sheet structure in the gel state. L-Phenylalanine and L-tyrosine containing tripeptides formed helical aggregates with handedness opposite to those containing L-valine and L-leucine residues. The mechanical stability of the hydrogels was found to depend on the hydrophobicity of the side chain of the tripeptide as well as on the pH of the solution. Also, the tripeptides exhibit in vitro proteolytic stability against proteinase K enzyme.

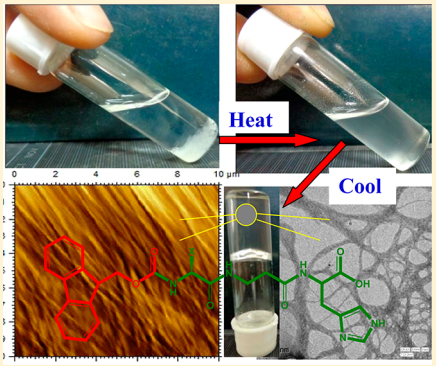

1. INTRODUCTION

In the past two decades, supramolecular self-assembly has stimulated research efforts on the rational design of smart materials that could provide robust routes for the development of a myriad of applications in the biomedical field. Hydrogels are a fascinating self-assembly system that are useful in biosciences because of their enormous use in regenerative medicine,[1] drug delivery,[2] biosensing,[3] 3-dimensional (3D) matrices for cell culture,[4] etc. A typical hydrogelator is a combination of two parts: the hydrophilic part enhances the solubility by interacting with water; the hydrophobic part encourages the molecules to aggregate in order to minimize their exposure to water. Driven by several noncovalent forces, such as hydrogen-bonding (H-bonding), $\pi-\pi$ stacking, and van der Waals interactions, the 3D elastic networks imbibe very large amounts of liquid (water, in case of hydrogels) in their interstitial spaces.[5−9] Among these materials, low-molecular-mass gelators (LMMGs) comprised of amino acid/peptides are one of the most common classes of hydrogelators owing to their easy synthesis and synthetic diversity, availability, and low cost.[10] In recent years, hydrogels based on short peptide-based gelators have found uses in applications such as wound healing, sustained release of drugs and biomolecules, pollutant removal from water, etc.[11−17] For peptide-based hydrogelators, the contribution of $\pi-\pi$-stacking interactions of the aromatic groups has been observed as one of the most important driving forces for efficient hydrogelation. Accordingly, in the design of new aromatic peptide-based building blocks that could configure highly stable self-associated systems, the *N*-fluorenylmethoxy-carbonyl (Fmoc) group is the most utilized functionality because of its rigid linker that offers sufficient length for effective self-assembly among aromatic and peptide domains.[18] Initially in 1995, Vegners et al. showed the hydrogelation by a Fmoc protected dipeptide.[19] Subsequently, efforts have been devoted by a number of groups to synthesize and develop new, N-terminally conjugated small molecular hydrogelators.[20−37] Phenylalanine has been shown to have a significant effect on hydrogelation.[35] Ulijn and co-workers demonstrated the propensity of Fmoc-diphenylalanine hydrogels to adopt β-sheet-type H-bonding networks through antiparallel, π-stacking interactions of the Fmoc groups.[35] Later, Nilsson and co-workers exploited the hydrogelation

Received: August 25, 2017
Revised: October 19, 2017
Published: October 24, 2017

DOI: 10.1021/acs.langmuir.7b03018
Langmuir 2017, 33, 12989−12999

ability of a hydrogelator consisting of Fmoc-protected pentafluorophenyl alanine (Fmoc-F_5-Phe). The highly fluorinated molecules, Fmoc-F_5-Phe, are much more efficient hydrogelators than the nonfluorinated analogue, Fmoc-Phe.[37] More recently, the same group explored the effect of the structure of benzyl side chains on the efficiency of the hydrogelators by incorporating electron-donating or electron-withdrawing groups.[38]

Although research on peptide-based hydrogelators (mainly containing α-amino acid residues) offers many avenues for investigation of supramolecular self-assembly, some limitations do exist in the scope of application of such types of peptides because of their susceptibility toward in vivo, proteolytic, enzyme-catalyzed hydrolysis. The inherent propensity of these peptide-hydrogelators toward proteolytic enzymes reduces their potency as drug carriers by shortening their lifetime inside the cell.[39,40] Therefore, to avoid such undesired effects by enzymes, an alternative approach to proteolytically stable hydrogelators that may mimic the functions of a peptide has been introduced. For example, introduction of a β- or D-α-amino acid residue into these peptide hydrogelators has attracted a great deal of attention. However, despite rapid progress in the development of β-amino acid- or D-α-amino acid-containing hydrogelators, only a few examples are known so far.[24,41−48] To address this issue further, we have developed a series of β-alanine-containing tripeptidic hydrogelators (see Chart 1 for structures)

Chart 1. Chemical Structure of Different Hydrogelators and L-Carnosine (Car)

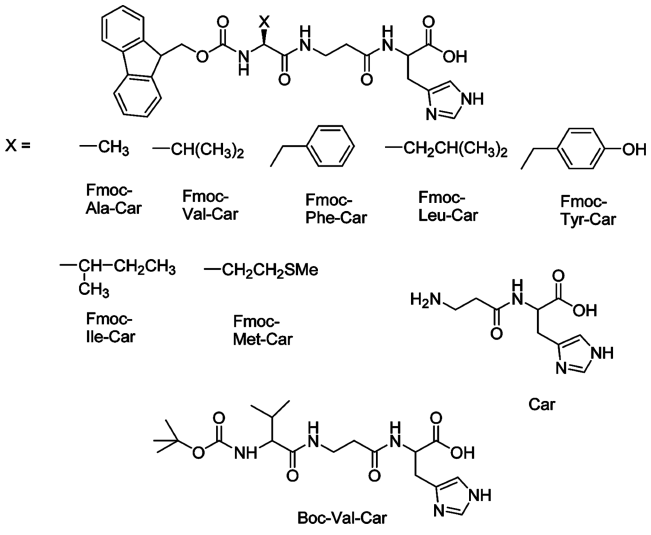

based on L-carnosine (Car), which is known to be involved in a number of biological activities. Car is a dipeptide of L-histidine and β-alanine. The β-alanine residue in Car plays a crucial role in its antioxidant properties for carbohydrates (antiglycation) and lipids (antilipoxidation).[49,50] Also, the L-histidine residue exhibits binding affinity toward transition metal ions. Because of the presence of the histidine residue, Car has the ability to inhibit glycation-induced protein cross-linking and has been prescribed to treat Alzheimer's disease.[51] Although the dipeptide has a number of biological activities, the gelation properties of its derivatives have not been explored widely. In fact, only two reports on the hydrogelation abilities of the derivatives of Car have appeared.[24,45] Keeping this in mind, we have synthesized seven Fmoc-tripeptides by covalently linking Fmoc-protected amino acids to Car and have investigated their self-assembly and hydrogelation properties by use of various techniques, including UV−vis, fluorescence, Fourier transform infrared (FTIR), circular dichroism (CD), and wide-angle X-ray diffraction (WAXD) spectroscopy, transmission electron microscopy (TEM), field emission scanning electron microscopy (FESEM), and atomic force microscopy (AFM) imaging, and rheology.

2. EXPERIMENTAL SECTION

2.1. Materials. L-Carnosine (99%) was purchased from Sigma-Aldrich (Bangalore, India). Fmoc-L-alanine (Fmoc-Ala) (98%), Fmoc-L-valine (Fmoc-Val) (98%), Fmoc-L-leucine (Fmoc-Leu) (98%), Fmoc-L-isoleucine (Fmoc-Ile) (98%), Fmoc-L-methionine (Fmoc-Met) (98%), Fmoc-L-phenyl alanine (Fmoc-Phe) (98%), Fmoc-tyrosine (Fmoc-Tyr) (98%), Boc-L-valine (Boc-Val) (98%), *N*-hydroxysuccininimide (NHS) (98%), 1,3-dicyclohexylcarbodiimide (DCC), proteinase K, and sodium hydroxide were purchased from SRL (Mumbai, India) and were used as received. All the organic solvents used for purification through column chromatography were of the highest purity (99%). Dichloromethane was dried by using CaH_2, and methanol was dried by using I_2/Mg turnings. Milli Q water (18 MΩ cm^{-1}) was used for the preparation of buffers.

All seven Fmoc-tripeptides considered in this study were synthesized in the laboratory. The *N*-protected tripeptides Fmoc-Ala-Car, Fmoc-Val-Car, Fmoc-Leu-Car, Fmoc-Ile-Car, Fmoc-Met-Car, Fmoc-Phe-Car, and Fmoc-Tyr-Car were obtained from Car by covalently linking an Fmoc-protected L-alanine (Fmoc-Ala), L-valine (Fmoc-Val), L-leucine (Fmoc-Leu), L-isoleucine (Fmoc-Ile), L-methionine (Fmoc-Met), L-phenyl alanine (Fmoc-Phe), and L-tyrosine (Fmoc-Tyr), respectively, by standard procedure.[52] The Boc-protected Boc-Val-Car was also synthesized by conjugating Boc-L-valine (Boc-Val) to Car following a similar procedure. The details are described under Supporting Information. The Fmoc-tripeptides were isolated in the neutral form as precipitates. The chemical structure of the Fmoc-tripeptides was identified by FTIR, ^{1}H NMR, and high-resolution mass spectra (HRMS) (see Figures S1 to S8).

2.2. Methods and Intrumentation. The melting point of the Fmoc-tripeptides was measured using Instind (Kolkata) melting point apparatus with open capillaries. The FTIR spectra were recorded with a PerkinElmer (model Spectrum Rx I) spectrometer. The ^{1}H and ^{13}C NMR spectra were recorded on an AVANCE DAX-400 (Bruker, Sweden) 400 MHz NMR spectrometer in DMSO-d_6 solvent.

Aqueous buffers (20 mM) in the pH range of 2−10 were used for the gelation studies. Buffers of pH 2 and pH 3 were prepared by mixing appropriate volumes of H_3PO_4 and NaH_2PO_4 solutions. Acetate buffers of pH 4 and 5 used for the study were prepared by mixing appropriate volumes of CH_3COOH and CH_3COONa solutions. Buffer solutions of pH 6, 7, and 8 were made by mixing appropriate volumes of NaH_2PO_4 and Na_2HPO_4 solutions. For the preparation of pH 9 and 10, carbonate buffers were employed. The pH was measured using a digital pH meter (Systronics-335, Kolkata, India) after standardizing the instrument with standard pH 7 and pH 4 buffers.

The gelation tests were performed in 20 mM aqueous buffer at different pH values. A weighed amount of the gelator, suspended in appropriate buffer in a screw-capped glass vial (o.d. ∼ 1 cm), was heated in a hot water bath (maintained at ∼80 °C) for 10−15 min to obtain a clear solution. The hot solution was then cooled in a temperature-controlled water bath maintained at 25 ± 0.1 °C. A preliminary assessment of gelation was made if the suspension did not flow during more than 1 min under the force of gravity upon inversion of the vial.

Because of poor aqueous solubility of the gelators, all measurements involving hydrogels were carried out at a concentration equal to their respective CGC (critical gelation concentration) value. Melting temperature of the gels were measured by inverting the screw-capped vial containing the gel in a temperature-controlled water bath

DOI: 10.1021/acs.langmuir.7b03018
Langmuir 2017, 33, 12989−12999

(JULABO, model F12). The gel was slowly heated at a 1 °C/min until the gelated mass started to flow on tilting of the vial.

The UV−vis spectra of solutions (10^{-5} M) were recorded with a UV-2450 UV−vis spectrophotometer (Japan) in a quartz cuvette of path length 1 cm. Fluorescence spectral measurements were performed using a 1 cm^2 quartz cuvette on a LS-55 luminescence spectrometer (PerkinElmer, U.K.), equipped with a filter polarizer and a thermostatting cell holder. Each sample was equilibrated for 12 h before recording the spectrum. The excitation wavelength in all the cases was 262 nm and fluorescence was detected at the right angle.

The morphology of the hydrogels was determined through the TEM, FESEM and AFM. TEM images were taken with a transmission electron microscope (FEI-TECNAI G2 20S-TWIN, FEI) operating at an accelerating voltage of 120 kV. The hydrogels were drop-cast on the carbon-coated copper grid, and the samples were air-dried. For FESEM experiments, the hydrogel was placed on a piece of aluminum foil and was air-dried at room temperature. A layer of gold was sputtered on top to make a conducting surface, and finally the specimen was transferred onto the field emission scanning electron microscope (FESEM, Zeiss, Supra-40, Netherland), operating at 5−10 kV to get the micrograph. The AFM experiments were performed by placing a drop of solution of the gelator at its pregelation concentration on a freshly cleaved mica foil. The material was then allowed to dry at room temperature, and then the images were taken with an atomic force microscope (Agilent 5500). The images were captured in the tapping mode using a silicon probe cantilever (PPP-NCL, Nanosensors, Inc.) of 215−235 mm length, resonance frequency of 146−236 kHz, and a force constant of 21−98 N m^{-1}.

The CD spectra were measured on a Jasco J-815 (Japan) spectropolarimeter using quartz cells of 1 mm path length. Each spectrum was baseline-corrected using the appropriate reference solvent. Each sample was equilibrated for 12 h before recording the spectra.

The wide-angle WAXD spectra were recorded at room temperature on a X-ray diffractometer (Bruker AXS, Diffractometer D8, Germany) using Cu source (Cu Kα, λ = 1.5418 Å) and Ni filter at a scanning rate of 0.001 s^{-1} between 2 and 30°. The operating voltage and current of the instrument were 40 kV and 30 mA, respectively. The hydrogel samples prepared on a glass slide were dried in the air overnight before measurement.

The rheological measurements were performed on a Bohlin RS D-100 (Malvern, UK) rheometer using parallel-plate (PP-20, diameter 20 mm) geometry with a constant tool gap of 100 μm. The rheometer was fitted with a solvent trap and Peltier device that controls temperature within 25 ± 0.1 °C. All measurements were performed with a matured gel after 10 h of preparation. The preformed gel was scooped out from the wide mouth vial by use of a spatula without causing any damage to the gel structure and was placed on the rheometer plate. An equilibration time of 30 min was allowed for each sample before measurement. Oscillatory stress sweep measurements were carried out at a constant frequency of 1 Hz to obtain storage modulus (G') and loss modulus (G''). The frequency sweep measurements were carried out keeping the stress value constant [1 Pa for all samples, except Fmoc-Phe-Car (pH 7) and Fmoc-Met-Car (pH 7)], where the stress values were 10 and 0.1 Pa, respectively).

Chromatographic analyses of samples were performed at 25 ± 1 °C with a high-performance liquid chromatograph (HPLC) using solutions filtered through a 0.45 μm membrane filter. The samples (20 μL injected volume) were analyzed using a Shimadzu system (Kyoto, Japan) equipped with LC-20AT Prominence liquid chromatograph 13 pump, DGU-20A3 Prominence Degasser, CBM-20A Prominence communications bus module, SPD-20A Prominence UV/vis detector, LC solution software, and a rheodyne injector with a 100 μL loop. Separation was performed using a Phenomenex RP C18 column, 250 × 4.6 mm, 5 μm, and an isocratic mobile phase of 70:30 (v:v) MeOH:H_2O at a 1 mL/min flow rate. The eluate was monitored at 254 nm.

3. RESULTS AND DISCUSSION

3.1. Gelation Behavior. As initial screening tests, hot solutions of a hydrogelator were cooled slowly in a temperature-controlled water bath maintained at 25 °C. If they did not flow perceptibly, they were deemed gels (i.e., the "inversion test tube" method).[5] In many cases, quenching a sol in an ice-cold water bath (i.e., fast cooling) also produced gels. Photographs of the appearances of the hydrogels at different pH values are shown in (Figure S9), and the results are summarized in Table 1. The data in Table 1 indicate that gelation depends on the

Table 1. Gelation Properties of Different Tripeptides in Aqueous Buffer of Varying pH at Room Temperature[a]

	CGC (% w/v) (T_{gs}/°C)						
pH	Fmoc-Ala-Car	Fmoc-Val-Car	Fmoc-Leu-Car	Fmoc-Ile-Car	Fmoc-Met-Car	Fmoc-Phe-Car	Fmoc-Tyr-Car
2	P	0.26, Tp (78)	0.27, Tp (75)	I	0.31, Tp (68)	0.24, Tp (82)	I
3	P	I	0.29, Tp (45)	I	0.32, Tp (58)	0.30, Tp (55)	I
4	I	I	I	I	W	I	I
5	I	I	I	I	W	I	I
6	I	I	I	I	I	I	I
7	P	0.70, Tl	0.30, Tl (55)	I	0.36, Tp (66)	0.28, Tp (90)	I
8	S	0.69, Tl (M)	S	I	0.39, Tp (47)	0.49, Tp (W)	0.46, Tl (44)

[a]The number within the parentheses represents corresponding the T_{gs} value. I = Insoluble, P = Precipitate, S = Solution, Tp = Transparent gel, Tl = Translucent gel, O = Opaque gel, W = Weak gel, M-Metastable gel. The concentration of the samples other than the hydrogels was 2.5 mg/mL.

hydrophobicity of the side chain moiety of the Fmoc-protected α-amino acid: under the same preparation conditions, Fmoc-Phe-Car shows an excellent ability to form hydrogels at pH 7 as well as at pH 2, and it exhibits the lowest CGC value (~0.2% w/v) among the hydrogelators investigated. At the same pH, Fmoc-Leu-Car and Fmoc-Met-Car afforded hydrogels with comparatively higher CGC values. On the other hand, L-alanine-containing Fmoc-Ala-Car failed to gel aqueous buffer within the pH range investigated; a precipitation was observed after cooling to room temperature. Fmoc-Val-Car formed a transparent hydrogel at pH 2 and a translucent gel at pH 7 and 8. However, the hydrogel at pH 7 was metastable, and it transformed into a viscous solution within ca. 30 min. When self-assembly is sufficiently efficient to form interfibril, non-covalent cross-links and, thus, a 3D network, its stability depends on complementary fibril−fibril interactions. Thus, we hypothesize that the smaller side chains of Ala and Val do not support adequately the required association between fibrils.

It has been previously reported that Fmoc-Tyr conjugated peptides are more effective hydrogelators than Fmoc-Phe ones.[29] The observed difference may be associated with the hydrophobicity and ring structure of the amino acid side chains. However, in the present study, attempts to gelate water in the pH range of 2−7 were unsuccessful for the Fmoc-Tyr-Car tripeptide. Indeed, Fmoc-Tyr-Car was difficult to dissolve at any pH in this range either by heating or sonication. Thus, if the hydrogelator-hydrogelator interactions from H-bonding are too strong, gelation is again inhibited because precipitation prevails. Ancillary evidence for these assertions comes from the

DOI: 10.1021/acs.langmuir.7b03018
Langmuir 2017, 33, 12989−12999

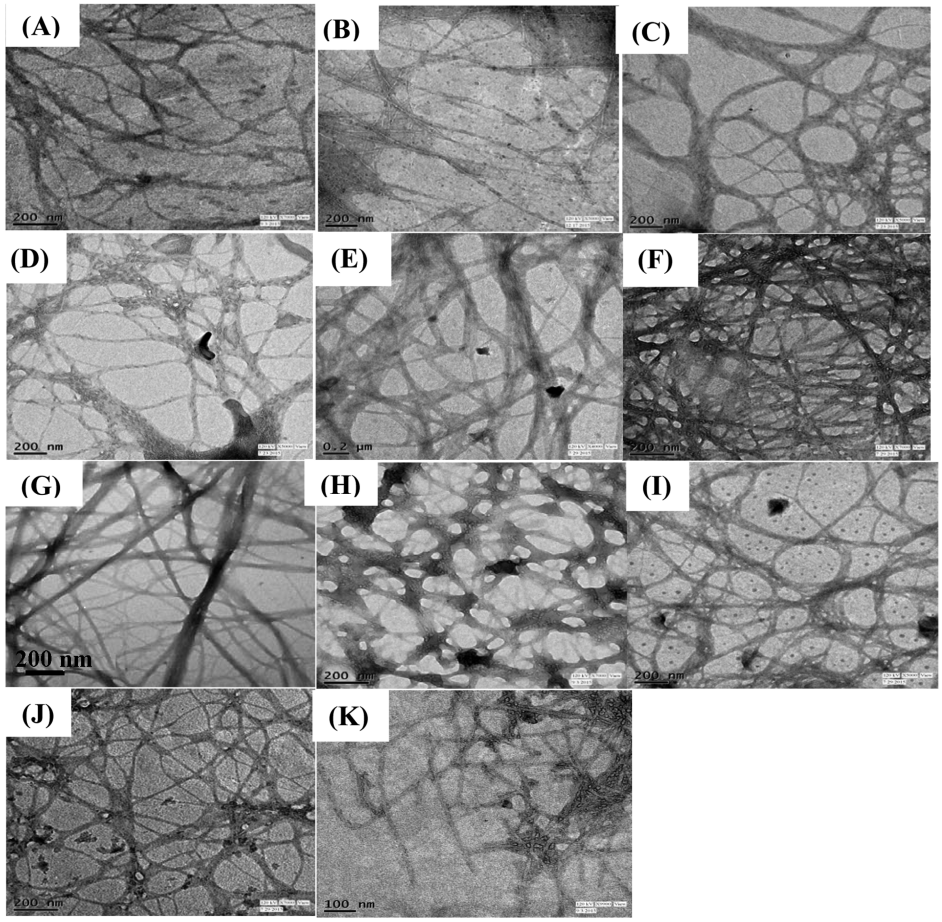

Figure 1. TEM images of the xerogels of (A) Fmoc-Val-Car (pH 2), (B) Fmoc-Val-Car (pH 7), (C) Fmoc-Leu-Car (pH 2), (D) Fmoc-Leu-Car (pH 7), (E) Fmoc-Met-Car (pH 2), (F) Fmoc-Met-Car (pH 7), (G) Fmoc-Met-Car (pH 5), (H) Fmoc-Ile-Car, (I) Fmoc-Phe-Car (pH 2), (J) Fmoc-Phe-Car (pH 7), and (K) Fmoc-Tyr-Car (pH 8).

high melting temperatures of the neat gelators (see Chemical identification); in these cases, the phenolic −OH group supplies the strong H-bonding interactions. However, at pH 8, after the suspended peptide had been heated and cooled, sonication for ∼3−5 min produced a homogeneous mixture, which on standing undisturbed for 5−6 h, afforded a translucent gel. At pH 9, however, all the peptides remained in solution, except Fmoc-Tyr-Car which dissolved only above pH 10. At pH 8, however, some of the peptides formed weak hydrogels. Therefore, for all the Fmoc-tripeptides, except Fmoc-Tyr-Car, only pH 2 and 7 were chosen for detailed investigation.

The above observations suggest that the interaction between side chains of neighboring gelator molecules plays a significant role in solubilization of the tripeptides and thus contributes importantly to the rigidity and stability of the hydrogels. A striking gelation behavior observed with Fmoc-Ile-Car further demonstrates the importance of side chain interaction during self-assembly formation: it remained insoluble in all buffer solutions at pH < 9, although the homologous Fmoc-Leu-Car efficiently formed a gel at pH 2 and 7. As noted, the side chain affects the packing of the gelator molecules in their neat solid states as well, as reflected by their melting temperatures. However, hydrophobicity of the side chains cannot explain the observed trend in gelation because it is very similar at pH 2. By contrast, the hydrophobicity of isoleucine is slightly higher than that for leucine (99 for isoleucine and 97 for leucine, considering 0 hydrophobicity for glycine) at pH 7.[53] Therefore, the presence of the methyl group in the side chain of the isoleucine derivative seems to be responsible for the difference in the behavior of these two gelators.

Previous reports have suggested that the gelation of peptide-based amphiphiles depends on the charge state of the C-terminal −COOH groups.[33] In order to investigate whether water alone at neutral pH could induce gelation, an equimolar amount of NaOH (relative to the Fmoc-Ile-Car monomer) was added to the peptide in water. Immediate solubilization was observed on slight heating, and subsequent addition of an equimolar amount of 1 (N) HCl turned the clear solution into an opaque gel.

The protonation−deprotonation behavior of the hydrogelators changes with the pH of the medium. The pK_a values of the imidazolium and −COOH groups of all the tripeptides were determined therefore by the pH titration method (see Figure S10). The pK_a values of the −COOH groups are in the range of 3.1 to 3.4, while those of the imidazoliums lie in the 6.8−7.1 region. These pK_a values agree well with those reported in the literature.[54] Thus, the pI values of the peptide gelators are ∼4.9, and both the imidazole ring of histidine and the free −COOH group existed in their protonated forms at pH 2. This facilitates intermolecular H-bonding interactions among gelator molecules. Indeed, the CGC value is observed to be lowest at pH 2. Because the hydrogelators remain mostly in their zwitterionic forms at 4 ≤ pH < 7 (due to deprotonation of

DOI: 10.1021/acs.langmuir.7b03018
Langmuir 2017, 33, 12989−12999

the −COOH groups), they are poorly soluble in water in this pH range and do not form gels. At pH ≥ 7, both the imidazole and −COOH groups are deprotonated, which helps solubilization and results in macroscopic gelation. Also, the presence of $-COO^-$ at pH ≥ 7 enhances the hydration by water and, thereby, reduces the gelation ability; at pH 7, Fmoc-Tyr-Car behaves in a similar fashion. Since the pK_a of deprotonation of the phenolic −OH group of L-tyrosine is ∼10.64,[55] it remains protonated at pH 7. However, the hydrogelator exhibits complete solubilization on sonication at pH 8, which is near its pK_a value. Fmoc-Tyr-Car, having slightly higher solubility at pH 8 than at pH 7, is gelated upon sonication.

Note that unlike dipeptide[25,27] and pentapeptide[28] gelators, the Fmoc-tripeptides exhibit neither salt-induced gelation nor increased stiffness upon addition of salt to a hydrogel. Instead, we observed precipitation of the gelators in the presence of inorganic salts (50 mM) such as NaCl, KCl, Na_2SO_4, and $CaCl_2$ at pH 2 and 7.

Comparison of the CGC values of all the hydrogelators provides information about the dependence of hydrogelation on the amino acid side chain. In fact, the hydrophobicity, additional π−π stacking interaction during self-assembly, and the charge state of the functional groups cumulatively determines the fate of the gelators and gelation. At pH 2, the hydrophobicity of the amino acid side chain decreases in the order Leu ∼ Ile > Phe > Val > Met > Tyr > Ala, whereas at pH 7, only Leu and Phe exchange their positions.[53] Therefore, Fmoc-Ala-Car failed to induce any gelation, and Fmoc-Tyr-Car had the highest CGC value. At both pH 2 and 7, the CGC value was next highest for Fmoc-Met-Car. Thus, except Fmoc-Phe-Car and Fmoc-Ile-Car, the gelation abilities in terms of CGC values follow the order of their hydrophobicity. Fmoc-Phe-Car, owing to its additional π−π-stacking, is the most effective hydrogelator at both pH values.

Furthermore, in order to examine the critical role of Fmoc group in the gelation process, a tripeptide Boc-Val-Car (see Chart 1) was synthesized by conjugating *N*-(tert-butoxycarbonyl)-L-valine (Boc-Val) to Car. As expected, the Boc-Val-Car failed to gelate pure water or at any of the pH values explored. Thus, the presence of the Fmoc group in these tripeptides plays an important role in the gelation process.

The thermo-reversibility as well as thermal stability test for the hydrogels was performed by measuring their gel-to-sol transition temperatures (T_{gs}). The T_{gs} values for different hydrogels were determined at their respective CGC values (Table 1). The results show that the hydrogel of Fmoc-Phe-Car at pH 2 and pH 7 are thermally the most stable, an observation attributed to the additional π−π stacking interaction between benzyl groups. Despite having the benzyl ring, the hydrogel of Fmoc-Tyr-Car at pH 8 shows a gel-to-sol transition at 44 °C due to the less efficient packing of this tripeptide molecule and the lower hydrophobicity of the Tyr moiety.

3.2. Morphology of the Hydrogels. *Scanning Electron Microscopy.* The formation of 3D network structures by the gelators in buffer is supported by the FESEM images of the corresponding xerogels as shown in Figure S11. The appearance of the self-assembled structures is consistent with the previously published images of peptidic hydrogelators.[35] The gel networks of the hydrogels were found to consist of bundles of entangled nanofibers of very high aspect ratio.

Transmission Electron Microscopy. Although the visual appearance on inversion of the vials indicated hydrogel formation by the tripeptides in the buffers, microscopic analysis of the hydrogels was carried out by TEM measurements as a means to obtain additional information about the networks (Figure 1). The results are consistent with those based on the FESEM images (Figure S11). All the images reveal network structures constituted by fibrils of different widths. The average fiber diameters (based on 3 observations) are collected in Table S1 for comparison purposes. As illustrated in Figure 1, the fibrils tend to be bundled under the conditions used for sample preparation. Because those conditions convert the gels into xerogels, it is not possible to assess the degree of fibril bundling in the actual gels. Regardless, the fibrillary nature of the gelator networks is established.

Although the Fmoc-Val-Car hydrogel shows a gel-to-sol transition within ca. 30 min of its preparation at pH 7, the sample appeared to have very thin, but few, fibers; an insufficient number of fibril−fibril interactions appears to be present in order to form a stable network. The TEM image of the self-assembled network structure of Fmoc-Ile-Car showed comparatively thicker aggregates with a higher number of junction jones. The degree of nanofiber bundling into thicker fibers, as observed from TEM images, was highest for Fmoc-Ile-Car. This morphological difference might be due to the difference in hydrophobicities of the Fmoc-L-amino acid residues, which influences the gelation process of Fmoc-Ile-Car as well, or to changes occurring as the water evaporates during sample preparation. The hydrogels of Fmoc-Met-Car at pH 7 exhibit a high degree of entanglement of fibers whose diameters are ca. 12 ± 2 nm (in contrast to ca. 25 ± 5 nm at pH 2). A similar type of self-assembled network for Fmoc-Phe-Car, with fibril diameters ca. 20 ± 3 and ca. 10 ± 4 nm, were also observed at pH 2 and pH 7, respectively. For all the gelators, the fibers were interconnected to create 3D gel networks and the fibrils that were up to several micrometres of length. The high aspect ratios of the gel fibers clearly suggest that the gelator−gelator intermolecular interactions are very anisotropic.[56] Since the gelator molecules are made of chiral amino acid residues, the primary and secondary aggregates of the gelators are expected to exhibit some form of helicity, as already reported for many gelator molecules.[21] However, none of the TEM images of the hydrogels reveals the existence of twisted fibers. This may be due to the methods used to prepare the samples for TEM or to the modes of gelator packing within the fibers.

AFM Images. In order to visualize finer details of the aggregates formed by the gelators, we examined AFM images of relatively concentrated dispersions of some representative gelators. The images of Fmoc-Phe-Car, Fmoc-Val-Car, Fmoc-Leu-Car, Fmoc-Met-Car, and Fmoc-Ile-Car tripeptides are presented in Figure S12. They show the existence of fiber-type aggregates of high aspect ratios, consistent with the TEM images. But it is interesting to observe that all the images exhibit helical or twisted ribbons (indicated by arrows). However, the low resolution of the images did not permit a detailed analysis of handedness or pitch.

3.3. Self-Assembly Studies. *Absorption Spectra.* The UV−vis absorbance spectra of the hydrogelators were measured in water at different pH values, and the results are summarized in Figure S13. For comparison purposes, the spectrum in the gel state of the Fmoc-Val-Car hydrogelator has also been included. All the spectra exhibited a strong band at ca. 206 nm, and weak absorption peaks in the region of 262−298 nm associated mainly with the π−π* transitions of the Fmoc chromophore. The absorption peaks in the region of 287−297

DOI: 10.1021/acs.langmuir.7b03018
Langmuir 2017, 33, 12989−12999

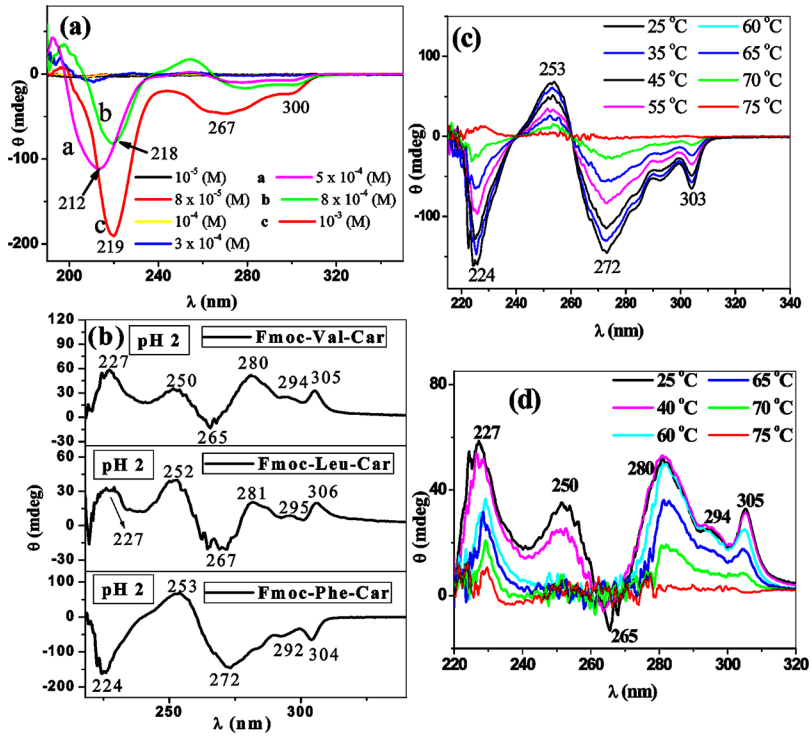

Figure 2. (a) CD spectra of Fmoc-Phe-Car at pH 7 at different concentrations. (b) CD spectra of different gelators in the gel state at pH 2. Variable temperature CD spectra of (c) Fmoc-Phe-Car (pH 2) and (d) Fmoc-Val-Car at pH 2. The gels were prepared at their respective CGC values. The path length of the cell was 1 mm.

nm of Fmoc-Val-Car in solution shifted to longer wavelengths in going from solution to the gel state (303 nm), suggesting formation of J-aggregates[57] through $\pi-\pi$ stacking interactions between Fmoc groups of neighboring molecules.

Fluorescence Spectra. Since fluorescence spectra are more sensitive than absorbance spectra to environmental change, steady-state fluorescence spectra (Figure S14) of the hydrogelators in dilute (10^{-6} M) aqueous solutions were recorded at both pH 7 and 2. The spectra exhibit a strong emission band at $\lambda_{max} \sim 315$ nm. The fluorescence spectra of two representative gelators Fmoc-Val-Car and Fmoc-Phe-Car were also recorded at higher concentrations in solution as well as in the gel state at both pH 7 and 2 (Figure S15). Increasing the gelator concentration results in a decrease of fluorescence intensity (due to high absorption of radiation near the cuvette surface or due to concentration quenching), along with a red shift of the emission maximum relative to dilute solutions. The red shift of the λ_{max} was largest in the gel state (337 nm), which is consistent with the absorption results, confirming strong $\pi-\pi$ stacking interactions among fluorenyl groups at higher concentrations.[35] For both gelators, the extent of red shift of the emission band at pH 7 (20 nm for Fmoc-Phe-Car) was greater than that at pH 2 (15 nm for Fmoc-Val-Car and 13 nm for Fmoc-Phe-Car). This indeed suggests that the degree of $\pi-\pi$ stacking interaction is stronger at pH 7 than that at pH 2. In addition to the short-wavelength fluorescence, the hydrogels of Fmoc-Phe-Car at pH 7 also exhibit a broad and weak emission band at ca. 455 nm (shown as inset of Figure S15) which results from extensive J-type aggregation of molecules through $\pi-\pi$ stacking interactions of either phenyl rings and/or Fmoc groups.[35]

3.4. Supramolecular Chirality. To envisage the backbone orientation of the peptides in the hydrogels and presence of chirality associated with self-association, CD spectroscopy is a useful tool and has been employed in the present study also. The molecular CD spectra of all the samples were recorded in the solution state at a gelator concentration equal to 1×10^{-4} M at which no significant self-association takes place (see SI) and also in the self-assembled hydrogel state (Figure 2). The CD spectra of the dilute solutions are presented in Figure S16. For comparison purposes, the CD spectrum of Car in phosphate buffer (pH 7) is also included in Figure S16. The corresponding HT (high tension voltage) data are presented in Figure S17 and Figure S18. As observed for Car, there are two positive CD bands at ca. 217 and 200 nm which correspond to the $\pi-\pi^*$ electronic transitions of the imidazole moiety and peptide bond, respectively. Similar positive CD bands were also observed with the gelators in their solution state. The results show that the gelators at pH 2 and 7 have either weak or no CD bands in the wavelength range between 240 and 320 nm, corresponding to the absorbance spectrum of Fmoc chromophore. In order to monitor the self-assembly process leading to supramolecular gelation, concentration-dependent CD spectra (Figure 2a) of Fmoc-Phe-Car, as a representative example, were measured at pH 7. As can be seen at [gelator] $\geq 5 \times 10^{-4}$ M, weak CD bands appear in the 240−320 nm regions. Further, the short wavelength band at 212 nm is observed to shift toward longer wavelengths in consistence with the UV−vis absorption spectra (Figure S13), indicating formation of J-aggregates. This is further supported by the results of fluorescence studies described above.

The CD spectra in the gel state of Fmoc-Val-Car, Fmoc-Leu-Car, and Fmoc-Phe-Car, as representative examples, are shown in Figure 2b. While Fmoc-Leu-Car and Fmoc-Val-Car hydrogels at pH 2 exhibit positive CD in the wavelength region 225−320 nm, the Fmoc-Phe-Car hydrogel at both pH 2 and 7

DOI: 10.1021/acs.langmuir.7b03018
Langmuir 2017, 33, 12989−12999

exhibits negative CD bands. Since only weak or no molecular CD is observed in the wavelength region 225−320 nm, the ellipticity in this range must arise from self-assembly formation in which fluorenyl groups are stacked face-to-face[35] and suggests superhelical arrangements of the peptide molecules during self-assembly formation.[36] It is important to note that along with an increase of ellipticity the molecular CD band (Figure S16) of Fmoc-Val-Car is red-shifted from 217 to 225 nm in the gel state of the tripeptide, indicating face-to-face stacking of the fluorenyl groups in the J-aggregates. Like Fmoc-Phe-Car, Fmoc-Tyr-Car also showed negative CD bands in the gel state. It is very important to note that this type of inversion is observed only with hydrogelators having phenyl group in the Fmoc-protected tripeptides. The inversion can be attributed to the change in the helical chirality of the fibrils relative to those observed with the other hydrogels.[32,35]

To further demonstrate the existence of helical aggregates in the gel state of the Fmoc-tripeptides, variable temperature CD spectra of the Fmoc-Val-Car and Fmoc-Phe-Car hydrogels were recorded. The results are presented in Figure 2 (panels c and d), which show progressive decrease of peak intensity on rising temperature with no CD signal above 225 nm at the highest temperature (75 °C). Thus, it is established that supramolecular structures leading to hydrogelation are largely temperature sensitive, and despite higher concentration, the sample did not exhibit any CD signal at higher temperature (75 °C), implying failure to produce any supramolecular chirality in dilute solution

3.5. Rheology of Hydrogels. In addition to visual observation of hydrogel formation by the tripeptides, rheological measurements were performed to confirm gelation and compare the mechanical strengths of different 3D network structures. All measurements were carried out at a [gelator] equal to their respective CGC value, and the results are shown in Figure S19 and Figure S20. The frequency (f) sweep measurements of all the hydrogels (Figure S19) indicate the storage modulus (G') and loss modulus (G'') remained nearly independent of f and $G' > G''$ over the experimental frequency range, suggesting formation of viscoelastic, soft solid-like gel material. In order to compare the rheological properties of the hydrogels, the rheological data including G' and G''/G' values are summarized in Table 2. Apparently, the rigidity of the hydrogels can be correlated from the frequency sweep experiment. In fact, the magnitude of G' denotes rigidity of the gel. The data suggest that Fmoc-Phe-Car hydrogels have the largest G' (>10^4 Pa) values compared to Fmoc-Tyr-Car. Fmoc-Ile-Car hydrogel also appeared with a very high G' value (>10^4 Pa).

Table 2. Rheological Parameters of Different Hydrogels at Different pHs at 25 °C

Hydrogelators	pH	G′ (Pa)	G″/G′	σ_y(Pa) ± 3 Pa
Fmoc-Val-Car	2	85	0.15	6
Fmoc-Leu-Car	2	1090	0.15	10
Fmoc-Met-Car	2	753	0.23	38
	7	31	0.39	8
Fmoc-Phe-Car	2	1143	0.14	107
	7	9300	0.21	747
Fmoc-Ile-Car	–	5200	0.14	108
Fmoc-Tyr-Car	8	10	0.11	8

The gel deformation study as a function of shear stress (σ) was performed to determine the mechanical stability of the hydrogels against stress. The data are presented in Figure S20. It is observed that after a certain stress value, the gel structure collapsed which defines the yield stress (σ_y) value. The σ_y values for different hydrogels are listed in Table 2. It is evident that Fmoc-Phe-Car hydrogel at pH 7 possessed the highest σ_y value and hence is the most stable. On the other hand, the Fmoc-Met-Car hydrogel appeared as the least stable. This can be attributed to the additional $\pi-\pi$ stacking interaction between adjacent phenyl rings, which is responsible for the increase of aspect ratio and hence greater entanglement of the fibers. However, it is important to note that although the gelation ability of Fmoc-Phe-Car is shown to be highest at pH 2 (with least CGC value), yet the mechanical stability of the hydrogel at pH 7 was observed to be highest. This is due to higher aspect ratio of the fibers at pH 7 in comparison to that at pH 2. This is reflected in the steady-state fluorescence spectra (Figure S15) of Fmoc-Phe-Car hydrogel at pH 7, which is more red-shifted (20 nm) relative to the solution spectrum in comparison to that at pH 2 (13 nm). This means $\pi-\pi$ stacking is facilitated more in pH 7 than in pH 2. Indeed the Fmoc-Phe-Car hydrogel at pH 7 exhibits an additional broad and weak emission band at ca. 455 nm; results indicative of extensive J-type aggregation of molecules through $\pi-\pi$ stacking interaction of either the phenyl ring and/or the Fmoc groups. However, no such broad emission peak was observed for the hydrogel at pH 2. The enhanced $\pi-\pi$ stacking interaction in the gel state at pH 7 is also indicated by the difference in T_{gs} values at different pHs (see Table 1).

The results of amplitude and frequency sweep measurements also reflect the effect of hydrophobicity of the side chain of the Fmoc-L-amino acid residue of the tripeptides. The hydrogels of gelators (e.g., Fmoc-Met-Car and Fmoc-Tyr-Car) with relatively less hydrophobic amino acid residue can be deformed easier than those with more hydrophobic residue. Owing to the presence of additional $\pi-\pi$ stacking interaction, the Fmoc-Phe-Car hydrogels emerged as the most stable. A similar conclusion has also been drawn by others for gelators containing aromatic moieties.[58] The mechanical stability of the hydrogels is also consistent with the thermal stability. This could be explained by the fact that the cross-linked fibers produced by less hydrophobic residues were easy to deform either thermally or mechanically by inhibiting strong fibril−fibril interaction.

3.6. Driving Forces for Gelation. *FTIR Spectra.* FTIR spectroscopy was used to probe the intermolecular interactions responsible for hydrogelation. The results are presented in Figure S21, and the spectral data are collected in Table S2. In the solid state, the peptides Fmoc-Phe-Car and Fmoc-Leu-Car displayed two peaks at 3405 $cm^{-1}$and 3297 cm^{-1} for Fmoc-Leu-Car whereas 3400 and 3298 cm^{-1} for Fmoc-Phe-Car, corresponding to stretching vibrations for O−H of carboxylic acid and N−H of amide group, respectively. In the xerogel state (pH 7), the amalgamation of these two peaks produced a broad peak at 3428 cm^{-1} for Fmoc-Leu-Car and 3422 cm^{-1} for Fmoc-Phe-Car, suggesting the participation of these bonds into hydrogel formation through H-bond formation. Two noticeable peaks at 1686 and 1647 cm^{-1} were also observed for the Fmoc-Phe-Car peptide in the solid state, which denotes carbonyl (C═O) stretching vibrations of acid and amide, respectively. In the xerogel state, broadening of the peaks with shifting to lower frequency region at 1639 cm^{-1} established the H-bonding between amide and acid groups during self-assembly

DOI: 10.1021/acs.langmuir.7b03018
Langmuir 2017, 33, 12989−12999

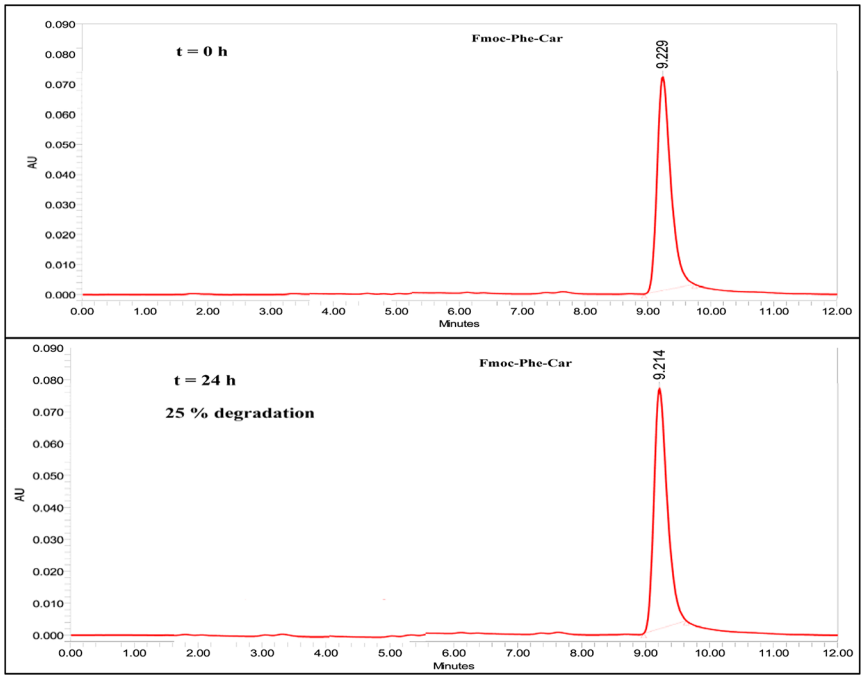

Figure 3. HPLC traces of the tripeptide Fmoc-Phe-Car after 0 and 24 h with proteinase K enzyme in HEPES buffer of pH 7.4.

formation. Moreover, the peak corresponding to N−H bending at 1541 cm^{-1} of Fmoc-Phe-Car in solid state almost disappeared in the xerogel state, which further supports the H-bond formation during self-assembly formation. A similar observation was also made with Fmoc-Leu-Car peptide in the gel state. Likewise, peptide Fmoc-Phe-Car in the solid state and in the xerogel state behaves in the similar fashion. A considerable shift of the O−H and N−H stretching vibrations (from 3400 to 3409 and 3317 to 3327 cm^{-1}, respectively) to higher frequency was observed in going from the solid to the xerogel state. A broad peak at 1637 cm^{-1} corresponding to C═O of the amide group was present in the xerogel state. Spectral shifts along with the broadening of peaks in the xerogel state compared to the solid state clearly confirmed participation of these groups in the H-bond network formation during gelation. Further the broad peak at 1637 cm^{-1} is indicative of an antiparallel β-sheet arrangement of the gelator molecules in the gel state.[35]

Wide Angle X-ray Diffraction Studies. WAXD is also a useful technique to observe molecular packing in the self-assembled state. For this, xerogels of Fmoc-Phe-Car, Fmoc-Leu-Car, and Fmoc-Val-Car at pHs 2 and 7 were prepared and WAXD measurements were performed with these samples. The results are shown in Figure S22, and the corresponding data are listed in Table S3. Hydrogel of Fmoc-Val-Car at pH 2 indicates the presence of two characteristic peaks at 2θ = 8.06° (d = 10.96 Å) and 2θ = 19.53° (d = 4.55 Å), which confirm presence of antiparallel β-sheet-like organization of the gelator molecules in the gel state.[13] The peak with d-spacing of 4.55 Å (2θ = 19.53°) implies the distance between the β-strands, and the peak at 2θ = 8.06° (d = 10.96 Å) suggests the distance between two β-sheets.[13] Moreover, the $\pi-\pi$ stacking arrangement can be confirmed from the characteristic peak at 2θ = 23.5° (d = 3.8 Å).[21] The WAXD spectra of Fmoc-Phe-Car at pH 2 and at pH 7 were also recorded, which show a similar type of diffraction pattern in the gel state. The characteristic peaks for $\pi-\pi$ stacking interaction are retained in the spectra of all the gelators employed, suggesting role of $\pi-\pi$ stacking interaction during self-assembly formation. However, it is important to note that the gelation mechanism, that is, the organization of the gelator molecules during gel formation, does not necessarily change with changing pH of the medium, since both the WAXD spectra of Fmoc-Phe-Car at pH 2 and pH 7 reveal similar types of peaks at the same position. This illustrates that the molecules prefer to orient in antiparallel β-sheet-type arrangement irrespective of pH of the medium.

3.7. Proteolytic Stability. As all the tripeptides contain one β-amino acid in their peptide sequence, hence it is expected that they might show resistance toward proteolysis upon treatment with proteolytic enzymes, such as proteinase K. To examine the proteolytic effect, tripeptides (1 mg/mL) were incubated in HEPES buffer (100 mM, pH 7.4) for 24 h in the presence of proteinase K at 37 °C. Then the respective control and incubated solutions were analyzed by HPLC. A representative chromatogram for the proteolysis of Fmoc-Phe-Car is shown in Figure 3. The results of other tripeptides are summarized in Figure S23. It is observed that after 24 h, there is no shift of the peak position but the peak area suffered only 22−27% reduction, suggesting only a minimum degradation of the tripeptides at physiological temperature and pH.[59] This suggests that the tripeptides are stable against proteolytic degradation, in vitro.

4. CONCLUSIONS

In summary, we have designed and developed seven Fmoc-tripeptide hydrogelators from L-carnosine by covalently linking different Fmoc-L-amino acids covering a range of side-chain hydrophobicities. These Fmoc-tripeptides show pH-sensitive hydrogelation in aqueous buffers at a relatively low concentration (<1% w/v), and their gelation abilities were observed to depend on the hydrophobicity of the side chain moiety of the Fmoc-L-amino acid residue. In contrast to previous reports,[29] the present study demonstrates that the L-phenylalanine-containing Fmoc-tripeptide exhibits highest

DOI: 10.1021/acs.langmuir.7b03018
Langmuir 2017, 33, 12989−12999

gelation ability among the amino acid residues examined. We associate this observation with the additional $\pi-\pi$ stacking interaction provided by the phenyl group. Although the same type of associative interaction is expected for the tyrosine residue, the gelation ability of the tyrosine-appended tripeptide was less as a result of strong intermolecular H-bonding interaction through the phenolic −OH group. Indeed, it has been shown by others also that although H-bonding interactions are known to enhance gelation ability, strong H-bonding reduces gelation ability of molecules.[60] Except in the case of Fmoc-Phe-Car, the efficiencies of hydrogelation followed the degrees of hydrophobicity of the side chain of Fmoc-protected α-amino acid. The Fmoc group was found to be important for hydrogelation. The Fmoc group played a major role in the formation of J-aggregates, the 1D growth of which produced fibrils of high aspect ratio. During self-assembly formation, the gelator molecules organize in an antiparallel β-sheet arrangement. The lamellar fibers thus formed undergo twisting to produce helical structures as indicated by CD spectra of the hydrogels of Fmoc-Val-Car, Fmoc-Leu-Car, and Fmoc-Phe-Car at both acidic and neutral pH. It is important to note that Fmoc-Phe-Car and Fmoc-Tyr-Car formed helical aggregates with handedness opposite that of the Fmoc-Val-Car and Fmoc-Leu-Car tripeptides. The Fmoc-Phe-Car and Fmoc-Ile-Car peptides were found to produce stronger hydrogels ($G' > 10^4$ Pa) compared to other Fmoc-protected dipeptides reported in the literature.[61,15] It is important to note that the mechanical strength of the hydrogels can be tuned by changing pH. Although it has been reported that gels can be prepared from dipeptide-gelators by salt addition, in the cases of Fmoc-tripeptides addition of salt was observed to cause precipitation of the gelator at room temperature. However, these hydrogelators were found to be proteolytically stable under physiological condition. As the hydrogels are thermally, mechanically, and proteolytically stable under physiological conditions, they can have potential use in biomedical applications.

■ ASSOCIATED CONTENT

Supporting Information

The Supporting Information is available free of charge on the ACS Publications website at DOI: 10.1021/acs.langmuir.7b03018.

Synthesis, chemical identification data, UV−vis, fluorescence, FTIR, HRMS, NMR, WAXD, and CD spectra, plots of pH titrations, HPLC data, FESEM and AFM images, tables of FTIR, TEM, and rheological data (PDF)

■ AUTHOR INFORMATION

Corresponding Author

*E-mail: joydey@chem.iitkgp.ernet.in. Fax: (+) 91-3222-255303.

ORCID

Joykrishna Dey: 0000-0002-6426-1109

Richard G. Weiss: 0000-0002-1229-4515

Notes

The authors declare no competing financial interest.

■ ACKNOWLEDGMENTS

We thank the Indian Institute of Technology Kharagpur for partial support of this work. R.D.M. thanks CSIR, New Delhi, for a research fellowship (09/081(1157)/2012-EMR-I). The authors are thankful to Mr. Kiran Patruni, Department of Agricultural Science, IIT Kharagpur, for his assistance with the rheological measurements.

■ REFERENCES

(1) Hirst, A. R.; Escuder, B.; Miravet, J. F.; Smith, D. K. High-Tech Applications of Self-Assembling Supramolecular Nanostructured Gel-Phase Materials: From Regenerative Medicine to Electronic Devices. *Angew. Chem., Int. Ed.* **2008**, *47*, 8002−8018.

(2) Vemula, P. K.; Li, J.; John, G. Enzyme Catalysis: Tool to Make and Break Amygdalin Hydrogelators from Renewable Resources: A Delivery Model for Hydrophobic Drugs. *J. Am. Chem. Soc.* **2006**, *128*, 8932−8938.

(3) Wada, A.; Tamaru, S.-i.; Ikeda, M.; Hamachi, I. MCM−Enzyme−Supramolecular Hydrogel Hybrid as a Fluorescence Sensing Material for Polyanions of Biological Significance. *J. Am. Chem. Soc.* **2009**, *131*, 5321−5330.

(4) Jayawarna, V.; Ali, M.; Jowitt, T. A.; Miller, A. F.; Saiani, A.; Gough, J. E.; Ulijn, R. V. Nanostructured Hydrogels for Three-Dimensional Cell Culture Through Self-Assembly of Fluorenylmethoxycarbonyl−Dipeptides. *Adv. Mater.* **2006**, *18*, 611−614.

(5) Terech, P.; Weiss, R. G. Low Molecular Mass Gelators of Organic Liquids and the Properties of Their Gels. *Chem. Rev.* **1997**, *97*, 3133−3160.

(6) Babu, S. S.; Praveen, V. K.; Ajayaghosh, A. Functional π-Gelators and Their Applications. *Chem. Rev.* **2014**, *114*, 1973−2129.

(7) Hamley, I. W.; Hutchinson, J.; Kirkham, S.; Castelletto, V.; Kaur, A.; Reza, M.; Ruokolainen, J. Nanosheet Formation by an Anionic Surfactant-like Peptide and Modulation of Self-Assembly through Ionic Complexation. *Langmuir* **2016**, *32*, 10387−10393.

(8) Zhang, M.; Xu, D.; Yan, X.; Chen, J.; Dong, S.; Zheng, B.; Huang, F. Self-Healing Supramolecular Gels Formed by Crown Ether Based Host−Guest Interactions. *Angew. Chem., Int. Ed.* **2012**, *51*, 7011−7015.

(9) Yan, X.; Xu, D.; Chi, X.; Chen, J.; Dong, S.; Ding, X.; Yu, Y.; Huang, F. A.Multiresponsive, Shape-Persistent, and Elastic Supramolecular Polymer Network Gel Constructed by Orthogonal SelfAssembly. *Adv. Mater.* **2012**, *24*, 362−369.

(10) Gao, Y.; Yang, Z.; Kuang, Y.; Ma, M. L.; Li, J.; Zhao, F.; Xu, B. Enzyme-instructed self-assembly of peptide derivatives to form nanofibers and hydrogels. *Biopolymers* **2010**, *94*, 19−31.

(11) Yang, Z.; Xu, K.; Wang, L.; Gu, H.; Wei, H.; Zhang, M.; Xu, B. Self-assembly of small molecules affords multifunctional supramolecular hydrogels for topically treating simulated uranium wounds. *Chem. Commun.* **2005**, 4414−4416.

(12) Yang, Z.; Liang, G.; Ma, M.; Abbah, A. S.; Lu, W. W.; Xu, B. D-Glucosamine-based supramolecular hydrogels to improve wound healing. *Chem. Commun.* **2007**, 843−845.

(13) Naskar, J.; Palui, G.; Banerjee, A. Tetrapeptide-Based Hydrogels: for Encapsulation and Slow Release of an Anticancer Drug at Physiological pH. *J. Phys. Chem. B* **2009**, *113*, 11787−11792.

(14) Xu, X.-D.; Liang, L.; Chen, C.-S.; Lu, B.; Wang, N.-l.; Jiang, F.-G.; Zhang, X.-Z.; Zhuo, R.-X. Peptide Hydrogel as an Intraocular Drug Delivery System for Inhibition of Postoperative Scarring Formation. *ACS Appl. Mater. Interfaces* **2010**, *2*, 2663−2671.

(15) Huang, R.; Qi, W.; Feng, L.; Su, R.; He, Z. Self-assembling peptide−polysaccharide hybrid hydrogel as a potential carrier for drug delivery. *Soft Matter* **2011**, *7*, 6222−6230.

(16) Rodríguez-Llansola, F.; Escuder, B.; Miravet, J. F.; Hermida-Merino, D.; Hamley, I. W.; Cardin, C. J.; Hayes, W. Selective and highly efficient dye scavenging by a pH-responsive molecular hydrogelator. *Chem. Commun.* **2010**, *46*, 7960−7962.

(17) Xu, H.; Das, A. K.; Horie, M.; Shaik, M. S.; Smith, A. M.; Luo, Y.; Lu, X.; Collins, R.; Liem, S. Y.; Song, A.; Popelier, P. L. A.; Turner,

M. L.; Xiao, P.; Kinloch, I. A.; Ulijn, R. V. An investigation of the conductivity of peptide nanotube networks prepared by enzyme-triggered self-assembly. *Nanoscale* **2010**, *2*, 960−966.
(18) Fleming, S.; Debnath, S.; Frederix, P. W. J. M.; Tuttle, T.; Ulijn, R. V. Aromatic peptide amphiphiles: significance of the Fmoc moiety. *Chem. Commun.* **2013**, *49*, 10587−10589.
(19) Vegners, R.; Shestakova, I.; Kalvinsh, I.; Ezzell, R. M.; Janmey, P. A. Use of a gel-forming dipeptide derivative as a carrier for antigen presentation. *J. Pept. Sci.* **1995**, *1*, 371−378.
(20) Vilaça, H.; Pereira, G.; Castro, T. G.; Hermenegildo, B. F.; Shi, J.; Faria, T. Q.; Micaêlo, N.; Brito, R. M. M.; Xu, B.; Castanheira, E. M. S.; Martins, J. A.; Ferreira, P. M. T. New self-assembled supramolecular hydrogels based on dehydropeptides. *J. Mater. Chem. B* **2015**, *3*, 6355−6367.
(21) Adhikari, B.; Nanda, J.; Banerjee, A. Multicomponent hydrogels from enantiomeric amino acid derivatives: helical nanofibers, handedness and self-sorting. *Soft Matter* **2011**, *7*, 8913−8922.
(22) Tang, C.; Ulijn, R. V.; Saiani, A. Effect of Glycine Substitution on Fmoc−Diphenylalanine Self-Assembly and Gelation Properties. *Langmuir* **2011**, *27*, 14438−14449.
(23) Orbach, R.; Adler-Abramovich, L.; Zigerson, S.; Mironi-Harpaz, I.; Seliktar, D.; Gazit, E. Self-Assembled Fmoc-Peptides as a Platform for the Formation of Nanostructures and Hydrogels. *Biomacromolecules* **2009**, *10*, 2646−2651.
(24) Castelletto, V.; Cheng, G.; Greenland, B. W.; Hamley, I. W.; Harris, P. J. F. Tuning the Self-Assembly of the Bioactive Dipeptide l-Carnosine by Incorporation of a Bulky Aromatic Substituent. *Langmuir* **2011**, *27*, 2980−2988.
(25) Roy, S.; Javid, N.; Frederix, P. W. J. M.; Lamprou, D. A.; Urquhart, A. J.; Hunt, N. T.; Halling, P. J.; Ulijn, R. V. Dramatic Specific-Ion Effect in Supramolecular Hydrogels. *Chem. - Eur. J.* **2012**, *18*, 11723−11731.
(26) Vilaça, H.; Hortelão, A. C. L.; Castanheira, E. M. S.; Queiroz, M.-J. R. P.; Hilliou, L.; Hamley, I. W.; Martins, J. A.; Ferreira, P. M. T. Dehydrodipeptide Hydrogelators Containing Naproxen N-Capped Tryptophan: Self-Assembly, Hydrogel Characterization, and Evaluation as Potential Drug Nanocarriers. *Biomacromolecules* **2015**, *16*, 3562−3573.
(27) Adams, D. J.; Mullen, L. M.; Berta, M.; Chen, L.; Frith, W. J. Relationship between molecular structure, gelation behaviour and gel properties of Fmoc-dipeptides. *Soft Matter* **2010**, *6*, 1971−1980.
(28) Kuang, Y.; Gao, Y.; Shi, J.; Lin, H.-C.; Xu, B. Supramolecular hydrogels based on the epitope of potassium ion channels. *Chem. Commun.* **2011**, *47*, 8772−8774.
(29) Sutton, S.; Campbell, N. L.; Cooper, A. I.; Kirkland, M.; Frith, W. J.; Adams, D. J. Controlled Release from Modified Amino Acid Hydrogels Governed by Molecular Size or Network Dynamics. *Langmuir* **2009**, *25*, 10285−10291.
(30) Yang, Z.; Liang, G.; Ma, M.; Gao, Y.; Xu, B. Conjugates of naphthalene and dipeptides produce molecular hydrogelators with high efficiency of hydrogelation and superhelicalnanofibers. *J. Mater. Chem.* **2007**, *17*, 850−854.
(31) Xing, B.; Yu, C.-W.; Chow, K.-H.; Ho, P.-L.; Fu, D.; Xu, B. Hydrophobic Interaction and Hydrogen Bonding Cooperatively Confer a Vancomycin Hydrogel: A Potential Candidate for Biomaterials. *J. Am. Chem. Soc.* **2002**, *124*, 14846−14847.
(32) Ryan, D. M.; Anderson, S. B.; Nilsson, B. L. The influence of side-chain halogenation on the self-assembly and hydrogelation of Fmoc-phenylalanine derivatives. *Soft Matter* **2010**, *6*, 3220−3231.
(33) Ryan, D. M.; Doran, T. M.; Anderson, S. B.; Nilsson, B. L. Effect of C-Terminal Modification on the Self-Assembly and Hydrogelation of Fluorinated Fmoc-Phe Derivatives. *Langmuir* **2011**, *27*, 4029−4039.
(34) Ryan, D. M.; Doran, T. M.; Nilsson, B. L. Stabilizing self-assembled Fmoc−F_5−Phe hydrogels by co-assembly with PEG-functionalized monomers. *Chem. Commun.* **2011**, *47*, 475−477.
(35) Smith, A. M.; Williams, R. J.; Tang, C.; Coppo, P.; Collins, R. F.; Turner, M. L.; Saiani, A.; Ulijn, R. V. Fmoc-Diphenylalanine Self Assembles to a Hydrogel via a Novel Architecture Based on $\pi-\pi$ Interlocked β-Sheets. *Adv. Mater.* **2008**, *20*, 37−41.
(36) Zhang, Y.; Gu, H.; Yang, Z.; Xu, B. Supramolecular Hydrogels Respond to Ligand-Receptor Interaction. *J. Am. Chem. Soc.* **2003**, *125*, 13680−13681.
(37) Ryan, D. M.; Anderson, S. B.; Senguen, F. T.; Youngman, R. E.; Nilsson, B. L. Self-assembly and Hydrogelation Promoted by F_5-Phenylalanine. *Soft Matter* **2010**, *6*, 475−479.
(38) Liyanage, W.; Nilsson, B. L. Substituent Effects on the Self-Assembly/Coassembly and Hydrogelation of Phenylalanine Derivatives. *Langmuir* **2016**, *32*, 787−799.
(39) Seebach, D.; Matthews, J. L. β-Peptides: a surprise at every turn. *Chem. Commun.* **1997**, 2015−2022.
(40) Jun, H.-W.; Yuwono, V.; Paramonov, S. E.; Hartgerink, J. D. Enzyme-Mediated Degradation of Peptide-Amphiphile Nanofiber Networks. *Adv. Mater.* **2005**, *17*, 2612−2617.
(41) Nanda, J.; Banerjee, A. β-Amino acid containing proteolitically stable dipeptide based hydrogels: encapsulation and sustained release of some important biomolecules at physiological pH and temperature. *Soft Matter* **2012**, *8*, 3380−3386.
(42) Garcia, A. M.; Kurbasic, M.; Kralj, S.; Melchionna, M.; Marchesan, S. A biocatalytic and thermoreversible hydrogel from a histidine-containing tripeptide. *Chem. Commun.* **2017**, *53*, 8110−8113.
(43) Liang, G.; Yang, Z.; Zhang, R.; Li, L.; Fan, Y.; Kuang, Y.; Gao, Y.; Wang, T.; Lu, B.; Xu, W. W. Supramolecular Hydrogel of a D-Amino Acid Dipeptide for Controlled Drug Release in Vivo. *Langmuir* **2009**, *25*, 8419−8422.
(44) Pal, A.; Dey, J. Rheology and thermal stability of pH-dependent hydrogels of N-acyl-L-carnosine amphiphiles: effect of the alkoxy tail length. *Soft Matter* **2011**, *7*, 10369−10376.
(45) Pal, A.; Shrivastava, S.; Dey, J. Salt, pH and thermoresponsive supramolecular hydrogel of N-(4-n-tetradecyloxybenzoyl)-L-carnosine. *Chem. Commun.* **2009**, 6997−6999.
(46) Castelletto, V.; Cheng, G.; Hamley, I. W. Amyloid peptides incorporating a core sequence from the amyloid beta peptide and gamma amino acids: relating bioactivity to self-assembly. *Chem. Commun.* **2011**, *47*, 12470−12472.
(47) Vargiu, A. V.; Iglesias, D.; Styan, K. E.; Waddington, L. J.; Easton, C. D.; Marchesan, S. Design of a hydrophobic tripeptide that self-assembles into amphiphilic superstructures forming a hydrogel biomaterial. *Chem. Commun.* **2016**, *52*, 5912−5915.
(48) Marchesan, S.; Styan, K. E.; Easton, C. D.; Waddington, L.; Vargiu, A. V. Higher and lower supramolecular orders for the design of self-assembled heterochiral tripeptide hydrogel biomaterials. *J. Mater. Chem. B* **2015**, *3*, 8123−8132.
(49) Brownson, C.; Hipkiss, A. R. Carnosine reacts with a glycated protein. *Free Radical Biol. Med.* **2000**, *28*, 1564−1570.
(50) Mehta, A. D.; Seidler, N. W. Beta-alanine suppresses heat inactivation of lactate dehydrogenase. *J. Enzyme Inhib. Med. Chem.* **2005**, *20*, 199−203.
(51) Hobart, L. J.; Seibel, I.; Yeargans, G. S.; Seidler, N. W. Anti-crosslinking properties of carnosine: significance of histidine. *Life Sci.* **2004**, *75*, 1379−1389.
(52) Becerril, J.; Bolte, M.; Burguete, M. I.; Galindo, F.; García-España, E.; Luis, S. V.; Miravet, J. F.Efficient Macrocyclization of U-Turn Preorganized Peptidomimetics: The Role of Intramolecular H-Bond and Solvophobic Effects. *J. Am. Chem. Soc.* **2003**, *125*, 6677−6686.
(53) Sereda, T. J.; Mant, C. T.; Sönnichsen, F. D.; Hodges, R. S. Reversed-phase chromatography of synthetic amphipathic α-helical peptides as a model for ligand/receptor interactions Effect of changing hydrophobic environment on the relative hydrophilicity/hydrophobicity of amino acid side-chains. *J. Chromatogr. A* **1994**, *676*, 139−153.
(54) Carnosine. http://www.druglead.com/cds/carnosine.html; accessed Nov 20, 2016.
(55) Amino Acids with Acidity Values http://academics.keene.edu/rblatchly/Chem220/hand/npaa/aawpka.htm; accessed Nov 20, 2016.
(56) Nanda, J.; Banerjee, A. β-Amino acid containing proteolitically stable dipeptide based hydrogels: encapsulation and sustained release

DOI: 10.1021/acs.langmuir.7b03018
Langmuir 2017, 33, 12989−12999

of some important biomolecules at physiological pH and temperature. *Soft Matter* **2012**, *8*, 3380−3386.
(57) Mishra, A.; Behera, R. K.; Behera, P. K.; Mishra, B. K.; Behera, G. B. Cyanines during the 1990s: a review. *Chem. Rev.* **2000**, *100*, 1973−2012.
(58) Yang, Z.; Wang, L.; Wang, J.; Gao, P.; Xu, B. Phenyl groups in supramolecular nanofibers confer hydrogels with high elasticity and rapid recovery. *J. Mater. Chem.* **2010**, *20*, 2128−2132.
(59) Baral, A.; Roy, S.; Ghosh, S.; Hermida-Merino, D.; Hamley, I. W.; Banerjee, A. A Peptide-Based Mechano-sensitive, Proteolytically Stable Hydrogel with Remarkable Antibacterial Properties. *Langmuir* **2016**, *32*, 1836−1845.
(60) Pal, A.; Dey, J. Water-Induced Physical Gelation of Organic Solvents by N-(n-Alkylcarbamoyl)-L-alanine Amphiphiles. *Langmuir* **2011**, *27*, 3401−3408.
(61) Tang, C.; Smith, A. M.; Collins, R. F.; Ulijn, R. V.; Saiani, A. Fmoc-Diphenylalanine Self-Assembly Mechanism Induces Apparent pKa Shifts. *Langmuir* **2009**, *25*, 9447−9453.

DOI: 10.1021/acs.langmuir.7b03018
Langmuir 2017, 33, 12989−12999